

Electronic Supplementary information

Manganese ions conjugated on layered bismuth oxyhalide for high-performance pseudo-capacitor and efficient oxygen evolution catalyst

Shiva Kumar Arumugasamy^a, Saravanan Govindaraju^{a,*}, Kyusik Yun^{a,*}

^a Department of Bionanotechnology, Gachon University, Gyeonggi-do, 13120, Republic of South Korea

Corresponding Author

*E-mail: biovijaysaran@gmail.com (S.G), ykyusik@gachon.ac.kr (K. Yun).

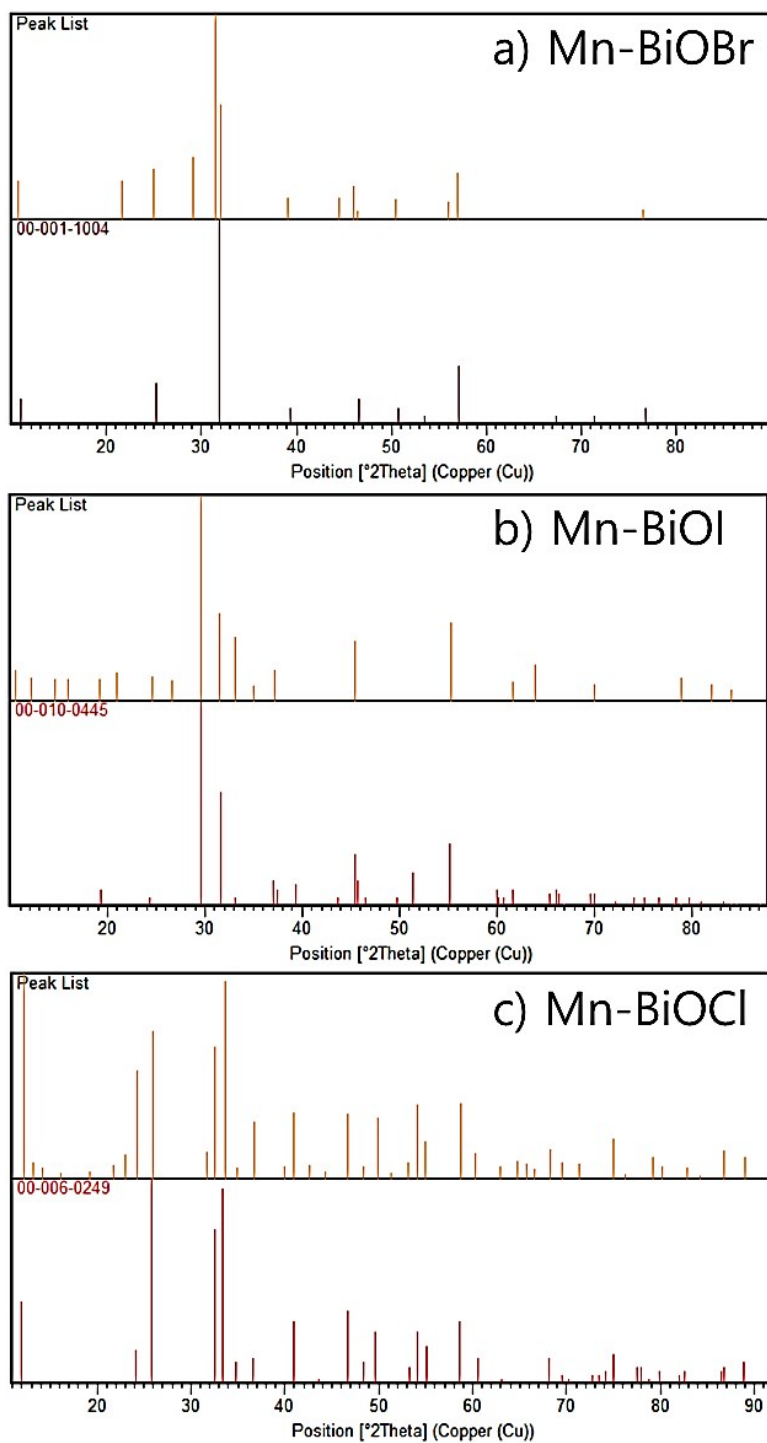


Fig. S1 Simulated XRD peak patterns for Mn-BiOX crystals.

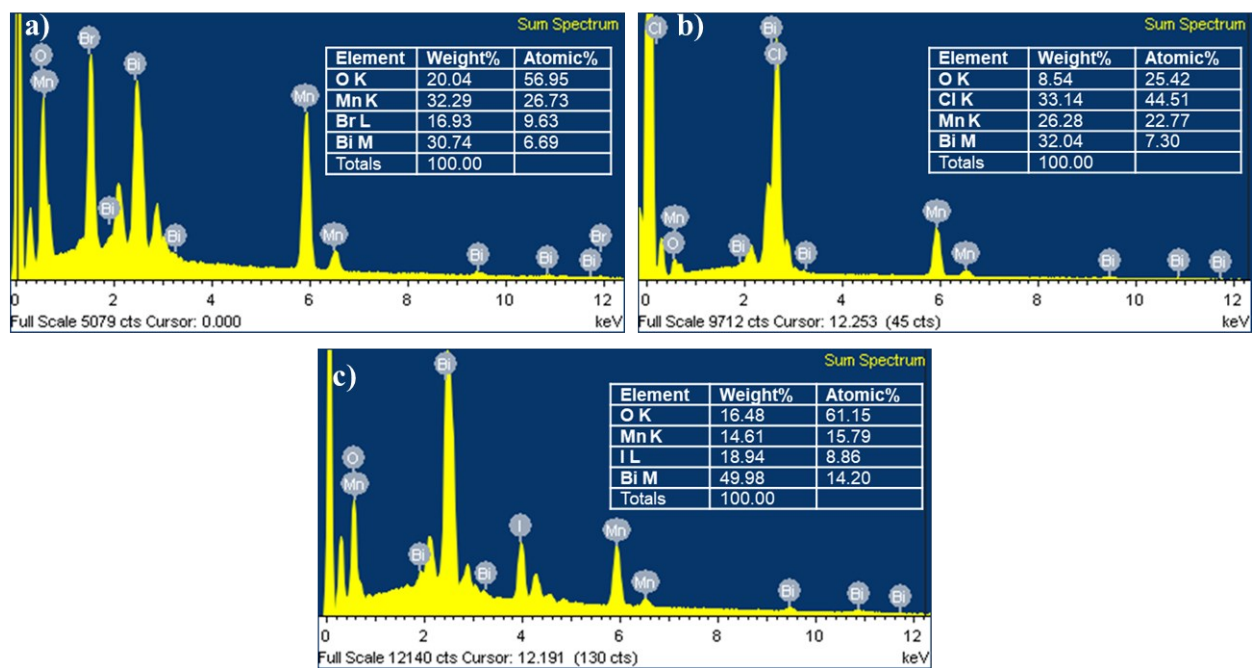


Fig. S2 EDS analysis for Mn-BiOX (X = Br, Cl and I) crystals.

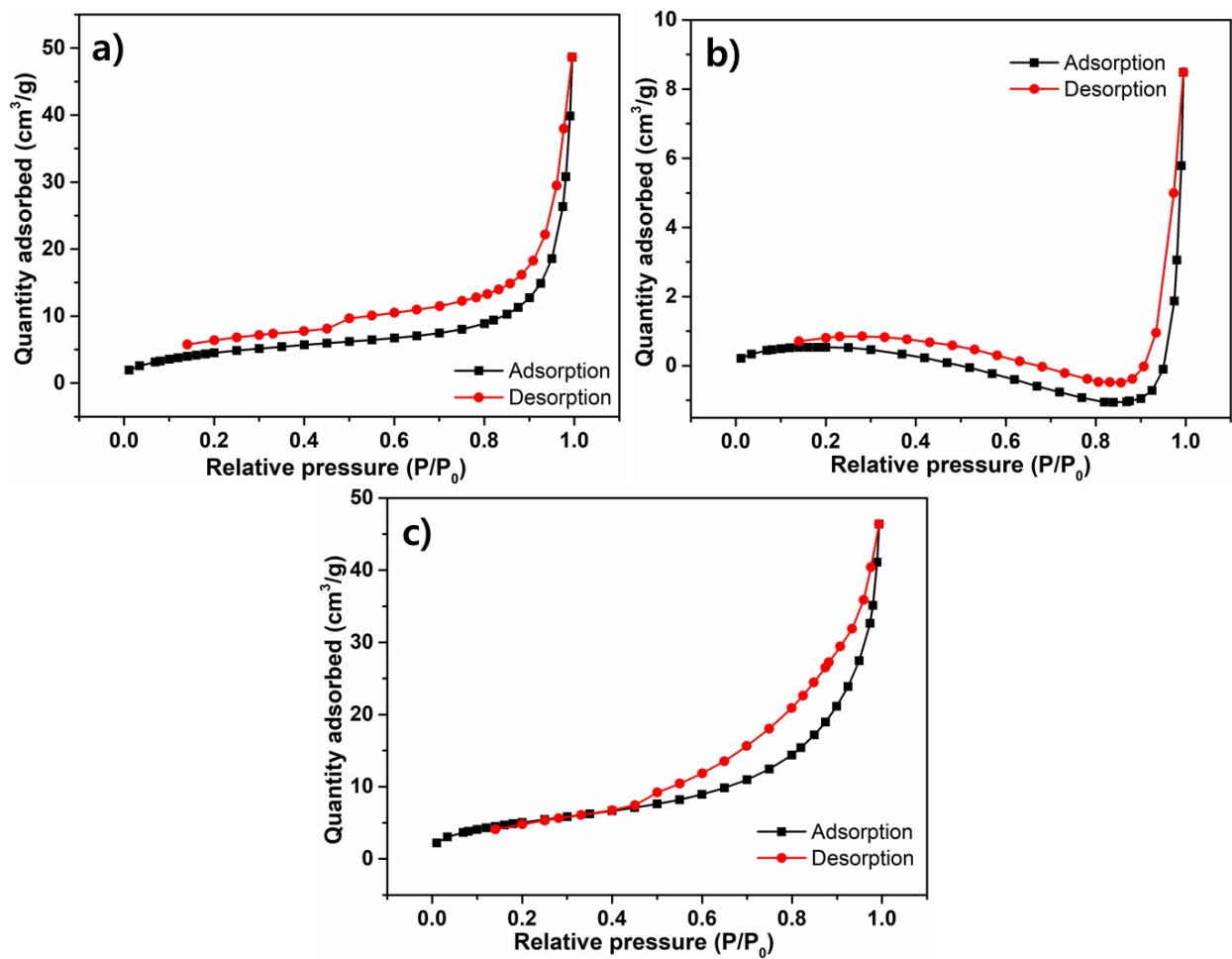


Fig. S3 Nitrogen adsorption-desorption isotherm of Mn-BiOX crystals (a: Mn-BiOBr, b: Mn-BiOI, and c: Mn-BiOCl).

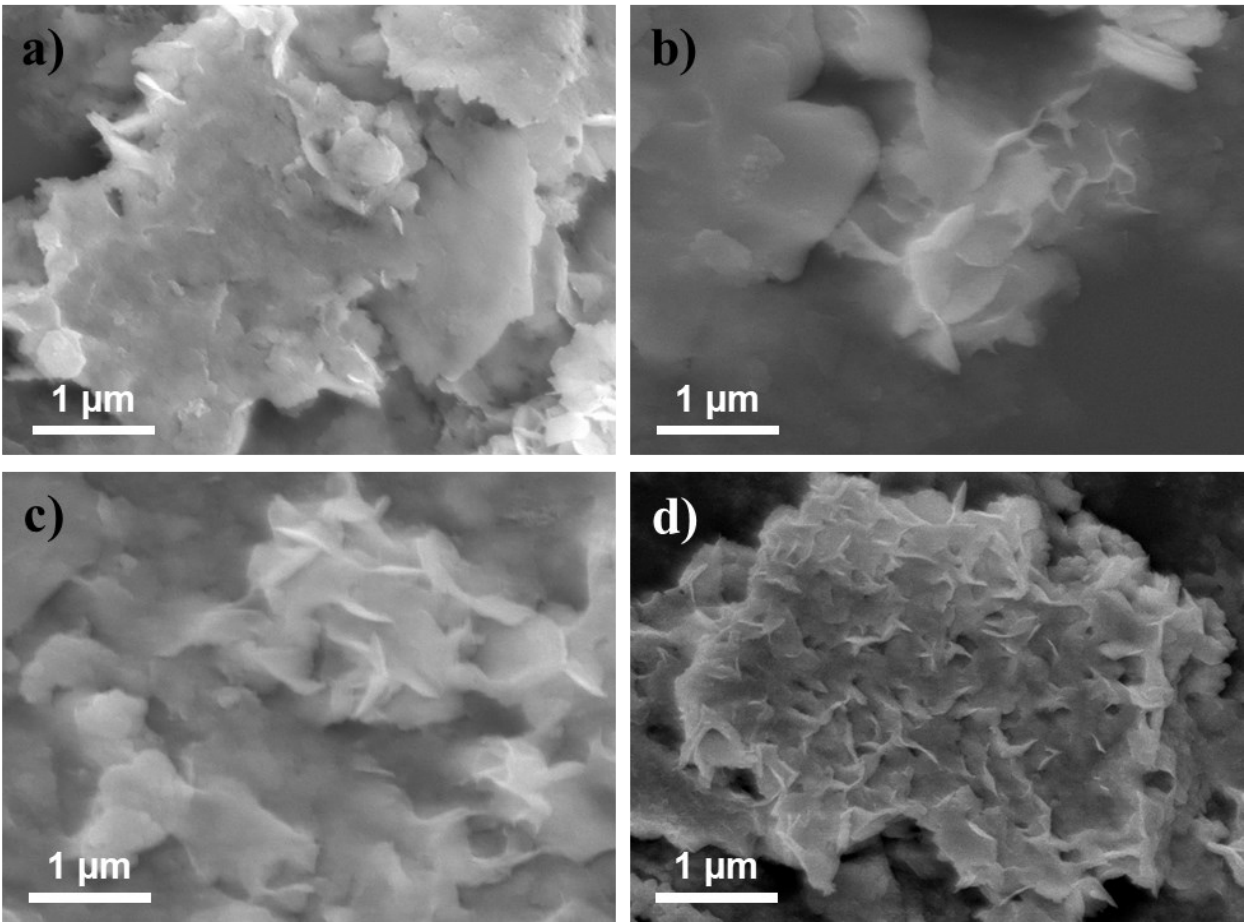


Fig. S4 FE-SEM images visualizing the growth mechanism of Mn-BiOCl material at various time intervals a) 1 h, b) 4 h, c) 8 h, and d) 12 h respectively.

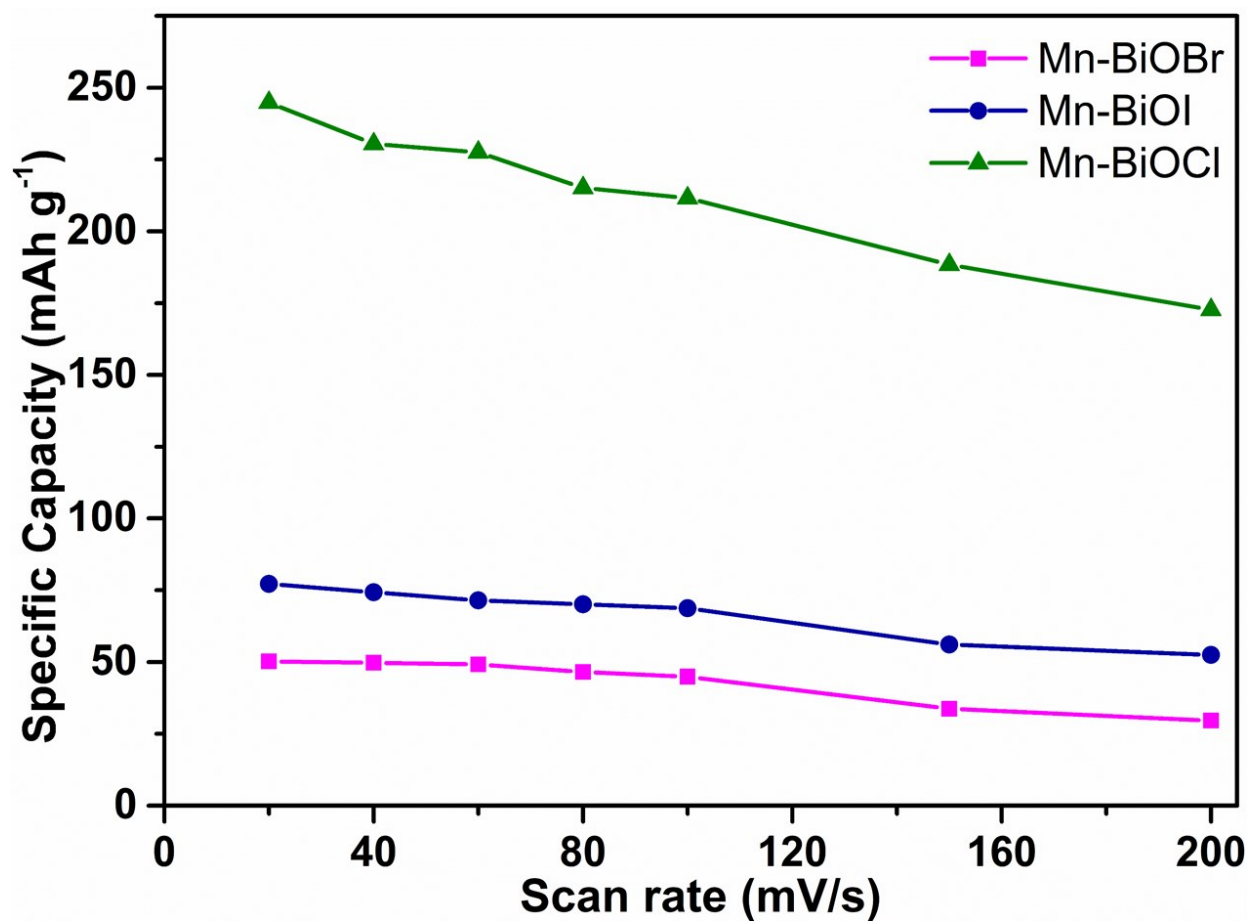


Fig. S5 Specific capacitance calculation through CV profiles for Mn-BiOX crystals.

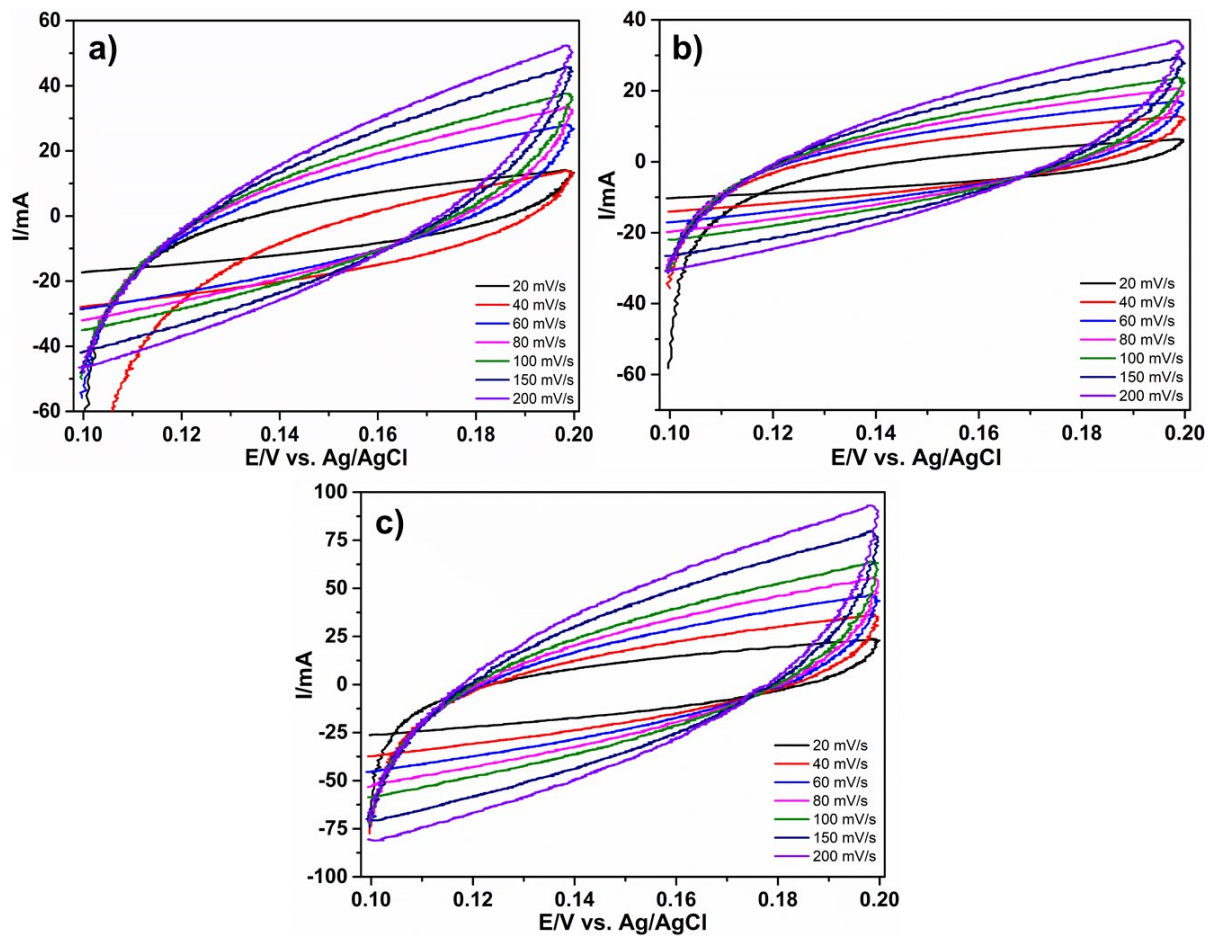


Fig. S6 CV profile for calculating double layer capacitance in the potential window of 0.1-0.2V using 1M KOH for the synthesized Mn-BiOX (X = Cl, Br, and I) materials.

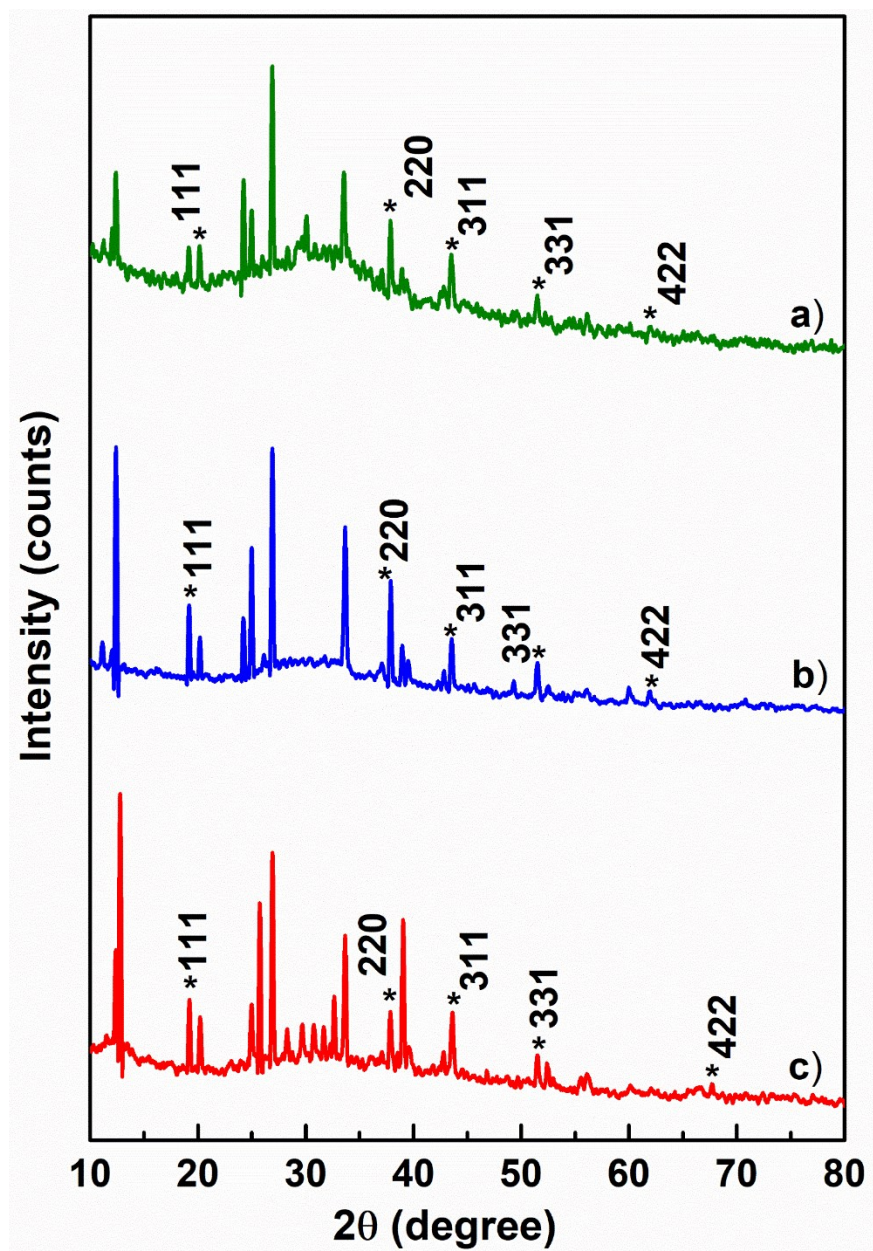


Fig. S7 XRD analysis after performing the chronoamperometric analysis for measuring the material stability (a: Mn-BiOBr, b: Mn-BiOI and c: Mn-BiOCl).

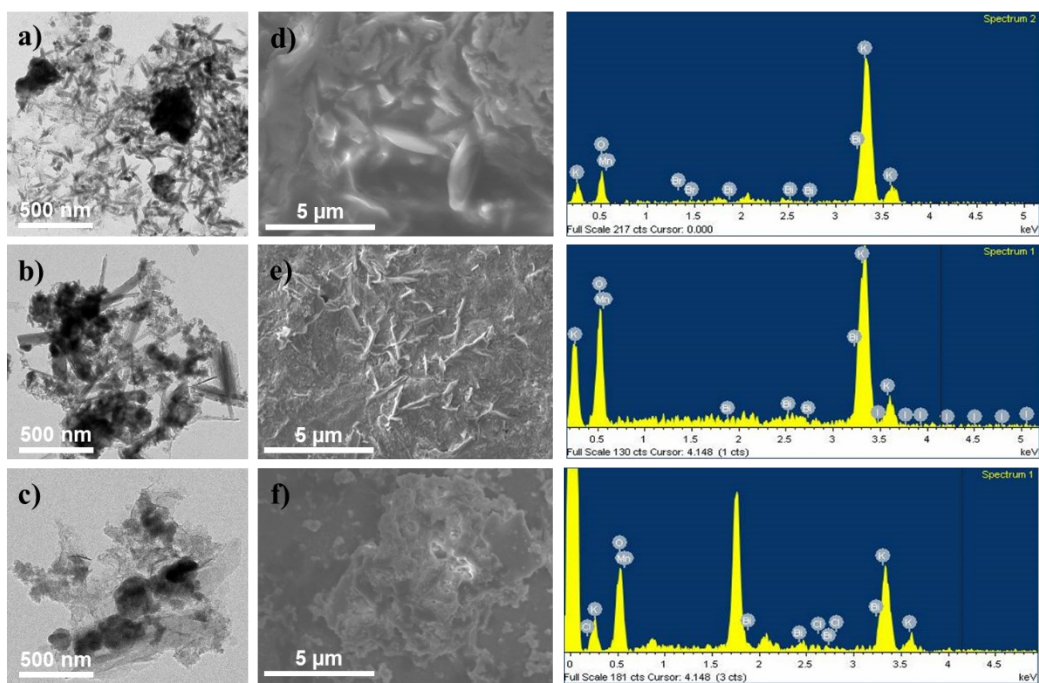


Fig. S8 TEM, FE-SEM and EDS analysis after performing the chronoamperometric analysis for measuring the material stability (a, d: Mn-BiOBr, b, e: Mn-BiOI and c, f: Mn-BiOCl)

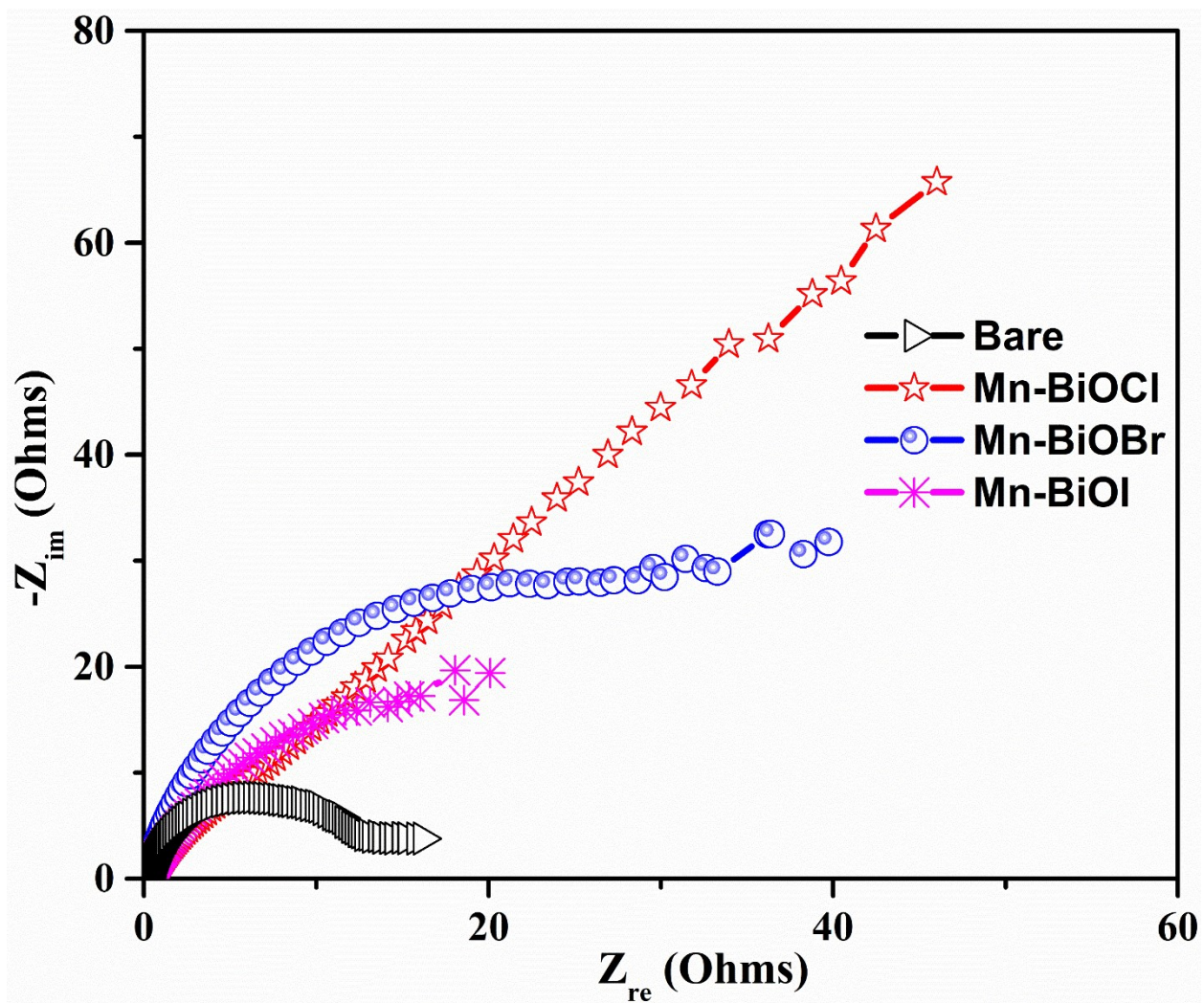


Fig. S9 Nyquist plot analysis after performing the chronoamperometric analysis for measuring the material stability.

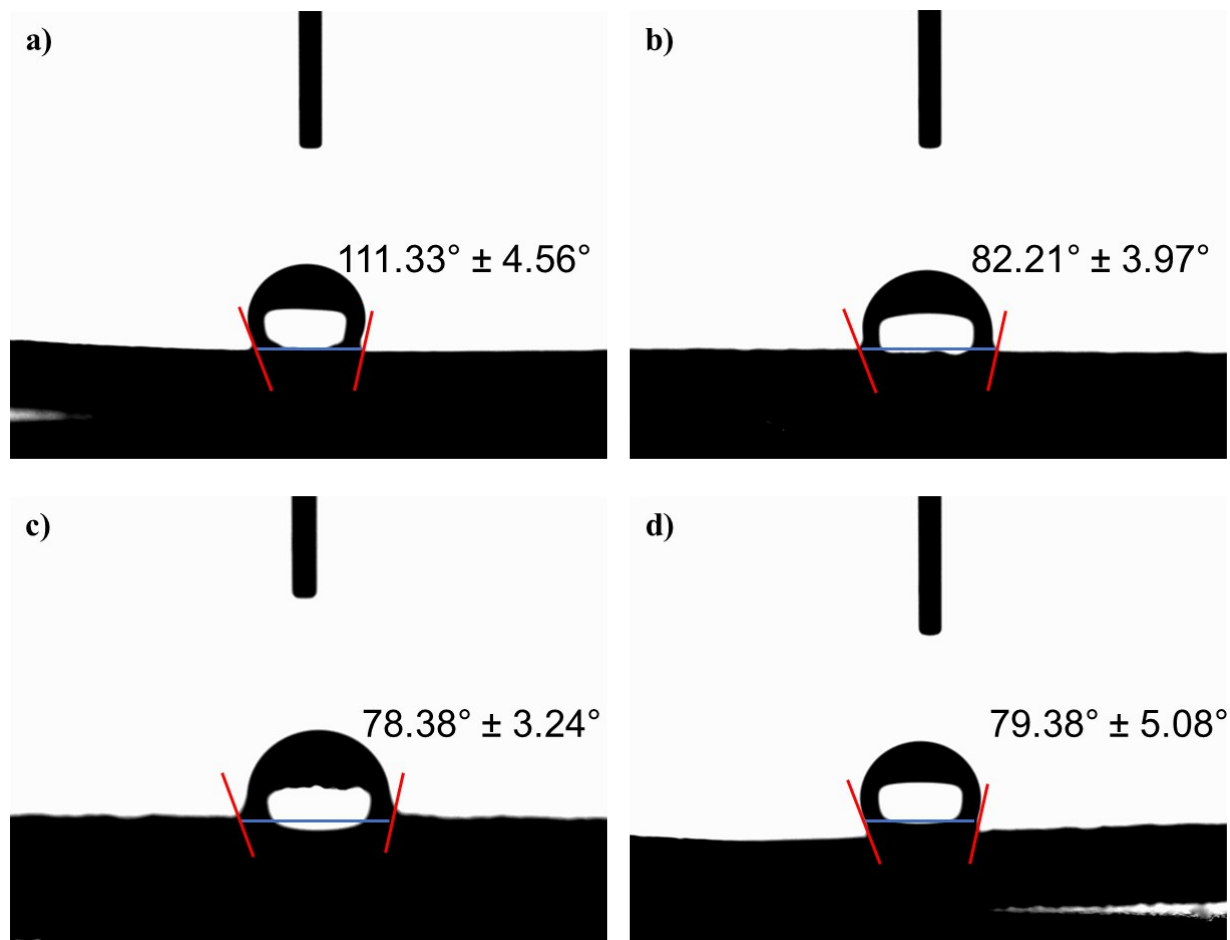


Fig. S10 Contact angle measurement strategy to determine the bonding nature between the electrode and synthesized materials a) bare electrode, b) Mn-BiOBr modified electrode, c) Mn-BiOCl modified electrode and d) Mn-BiOI modified electrode.

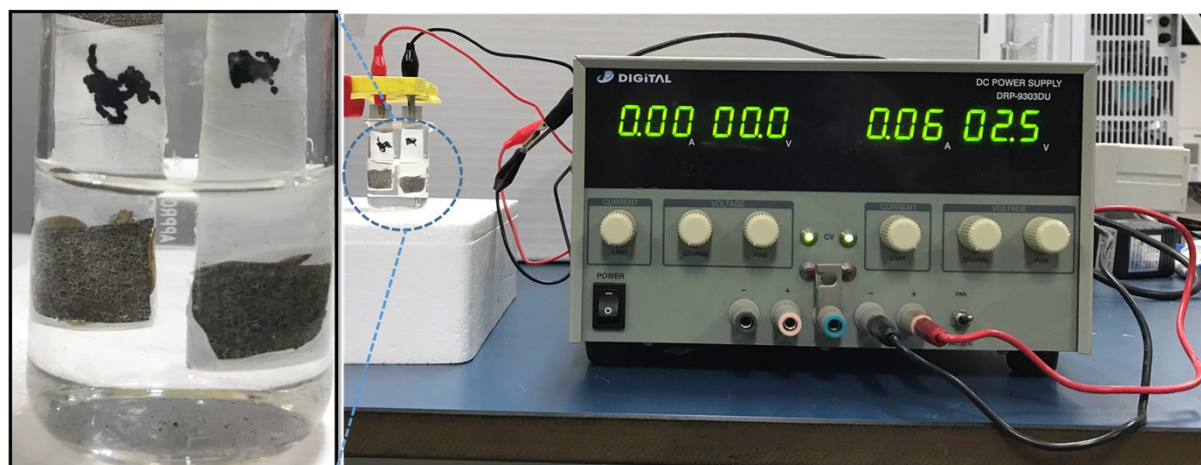


Fig. S11 Practical applicability of the synthesized materials.

Table. S1 Electrochemical Impedance spectroscopic values for Mn-BiOX (X= Br, I and Cl)

Electrode surface	Fitting Parameters			
	R_S (Ω)	C_{dl} (F)	R_{ct} (Ω)	Warburg (Ω)
Bare	2	5.421×10^{-6}	8	4.43×10^{-7}
Mn-BiOBr	3	2.142×10^{-7}	5	5.16×10^{-5}
Mn-BiOI	1.5	1.111×10^{-6}	3.5	5.08×10^{-5}
Mn-BiOCl	1	3.939×10^{-7}	2	1.72×10^{-5}

Table. S2 Comparative capacitance study analysis with other materials

S.No	Materials	SC (F/g)	ED (Wh/Kg)	PD (W/Kg)	Stability (%)	Ref
1.	BiOI/Bi ₉ I ₂	122.43	38.2	228.4	90.1	S1
2.	BiOCl/Fe(III)	540	17	500	72	S2
3.	BiOCl/MXene	247.8	15.2	567.4	57.5	S3
4.	Bi ₇ O ₉ I ₃	347	-	-	65.5	S4
5.	BiOI	706	-	-	55	S5
6.	BiOCl/AC	1243	17.2	250.9	90.3	S6
7.	BiOCl/PANi	169.9	-	-	-	S7
8.	Bi ₂ O ₃ -MnO ₂	161	18.4	600	95	S8
9.	Bi ₂ O ₃	322.5	7.2	334.7	92	S9
10.	Bi ₂ O ₃ /rGO	617.1	-	-	79.5	S10
11.	Mn-BiOBr	676.8	6.47	918.75	89.4	This Wor k
	Mn-BiOI	861.7	10.9	831.25	88.6	
	Mn-BiOCl	2291.3	25.77	1400	86.4	

Table. S3

S. No	Material	Electrolyte	Overpotential / mV	Tafel / mV dec ⁻¹	Reference
1.	Bi ₂ S ₃ /Ni ₃ S ₂	1M KOH	268	82	S11
2.	MA ₂ CoBr ₄	PBS	528	197	S12

3.	Fe _{1.75} Mn _{0.25} P	1M KOH	620	100	S13
4.	Mn-BiOCl	2M KOH	325	160	This work
	Mn-BiOI		378	192	
	Mn-BiOBr		485	214	

References

- S1. S. Park, N. M. Shinde, P. V. Shinde, D. Lee, J. M. Yun and K. H. Kim, Chemically grown bismuth-oxy-iodide (BiOI/Bi₉I₂) nanostructure for high performance battery-type supercapacitor electrodes, *Dalton Tran.*, 2020, **49**, 774-780.
- S2. R. Rameshbabu, M. Sandhiya and M. Sathish, Fe (III) ions grafted bismuth oxychloride nanosheets for enhanced electrochemical supercapacitor application, *J. Electroanal. Chem.*, 2020, **862**, 113958.
- S3. Q. X. Xia, N. M. Shinde, J. M. Yun, T. Zhang, R. S. Mane, S. Mathur and K. H. Kim, Bismuth Oxychloride/MXene symmetric supercapacitor with high volumetric energy density, *Electrochim. Acta*, 2018, **271**, 351-360.
- S4. P. Wu, L. Feng, Y. Liang, X. Zhang, X. Li, S. Tian, H. Hu, G. Yin and S. Khan, Large-scale synthesis of 2D bismuth-enriched bismuth oxyiodides at low temperatures for high-performance supercapacitor and photocatalytic applications, *J. Mater. Sci: Mater. Electron.*, 2020, **31**, 5385-5401.
- S5. S. Vadivel, B. Saravanakumar, M. Kumaravel, D. Maruthamani, N. Balasubramanian, A. Manikandan, G. Ramadoss, B. Paul and S. Hariganesh, Facile solvothermal synthesis of BiOI microsquares as a novel electrode material for supercapacitor applications, *Mater. Lett.*, 2018, **210**, 109-112.

- S6. W. Hong, L. Wang, K. Liu, X. Han, Y. Zhou, P. Gao, R. Ding and E. Liu, Asymmetric supercapacitor constructed by self-assembled camellia-like BiOCl and activated carbon microspheres derived from sweet potato starch, *J. Alloy. Compd.*, 2018, **746**, 292-300.
- S7. G. Nie, X. Lu, W. Wang, M. Chi, Y. Jiang and C. Wang, One-dimensional polyaniline thorn/BiOCl chip heterostructures: self-sacrificial template-induced synthesis and electrochemical performance, *Materials Chemistry Frontiers* 2017, **5**, 859-866.
- S8. S. Singh, R. K. Sahoo, N. M. Shinde, J. M. Yun, R. S. Mane and K. H. Kim, Synthesis of Bi₂O₃-MnO₂ Nanocomposite Electrode for Wide-Potential Window High Performance Supercapacitor, *Energies*, 2019, **17**, 3320.
- S9. R. C. Ambare, P. Shinde, U. T. Nakate, B. J. Lokhande and R. S. Mane, Sprayed bismuth oxide interconnected nanoplate supercapacitor electrode materials, *Appl. Surf. Sci.*, 2018, **453**, 214-219.
- S10. S. Liu, Y. Wang and Z. Ma, Bi₂O₃ with reduced graphene oxide composite as a supercapacitor electrode, *Int. J. Electrochem. Sci.*, 2018, **13**, 12256-12265.
- S11. S. Wang, W. Xue, Y. Fang, Y. Li, L. Yan, W. Wang and R. Zhao, Bismuth activated succulent-like binary metal sulfide heterostructure as a binder-free electrocatalyst for enhanced oxygen evolution reaction, *J. Colloid Interf. Sci.*, 2020.
- S12. R. Babu, A. K. Vardhaman, V. M. Dhavale, L. Giribabu and S. P. Singh, MA₂CoBr₄: lead-free cobalt-based perovskite for electrochemical conversion of water to oxygen, *Chem. Commun.*, 2019, **55**, 6779.
- S13. D. Li, H. Bayduon, B. Kulikowski and S. L. Brock, Boosting the catalytic performance of iron phosphide nanorods for the oxygen evolution reaction by incorporation of manganese, *Chem. Mater.*, 2017, **29**, 3048.